On Driving Non-passive Macromodels to Instability

On driving non-passive macromodels to instability

S. Grivet-Talocia

Dept. of Electronics, Politecnico di Torino, C. Duca degli Abruzzi 24, 10129 Torino, Italy
Tel: +39-011-564-4104, Fax: +39-011-564-4099, E-mail: grivet@polito.it

Revised paper n.2 – March 17, 2008

Abstract

This paper illustrates a procedure for demonstrating and quantifying the importance of passivity in linear macromodels. This issue is critical whenever the macromodels are derived from tabulated port responses, either in time or frequency domain. We show an algorithmic procedure for the design of a passive termination network that will drive to instability a given non-passive macromodel. Several termination structures characterized by various port couplings are investigated. Relaxed passivity conditions are also given that guarantee the stability of the macromodel under specific reduced-coupling loading conditions. Theoretical results are applied to a set of application test cases.

Keywords: Linear macromodeling, Passivity, Stability, Scattering.

1 Introduction

The design flow of digital and mixed-signal systems requires accurate Signal Integrity verifications. The influence of all system parts on signal quality must be carefully investigated using suitable predictive models in system-level simulations. These macromodels [1, 2] can be viewed as simple mathematical expressions providing an approximation of the frequency response of the structure under investigation, usually over a broad frequency spectrum. In this work, we concentrate on electrical interconnect structures, such as connectors or via arrays. The common approach for deriving models of such structures is to start with a brute-force full-wave solution of Maxwell equations (typically using commercial solvers) in order to derive tabulated frequency responses at selected ports. Alternatively, such responses may be obtained via direct measurement, if possible. In a second step, rational curve-fitting algorithms [3, 4] are applied, in order to produce a mathematical representation for the electrical behavior of the structure that is implementable as a lumped netlist. Finally, system-level simulations are carried out using standard circuit solvers such as SPICE. This equivalent circuit modeling approach is a standard practice in several different application areas (see, e.g., [5, 6]). Moreover, it generally provides

much higher efficiency than direct computation of discrete impulse responses from frequency samples followed by numerical convolution in time-domain [7].

Electrical interconnects are obviously passive, i.e., unable to generate energy, based on first principle physical considerations. Unfortunately, passivity may be lost in the macromodel either during the derivation of the raw frequency samples, as a result of numerical simulation or measurement/calibration errors, or during the curve-fitting phase. Loss of macromodel passivity implies that it is possible to find a termination circuit that drives the macromodel to instability. This result has been known since many years [8]-[21], mainly in application areas such as amplifier design, system theory and control. In such context, what we call here "macromodel" is either a system with an intended active behavior, typically amplifier circuits [12]-[21], or a "plant" to be controlled [22]. It is natural to expect possible instabilities in such systems if no proper countermeasures are taken. Various denominations such as *conditional stability*, *potential stability* or *potential instability* have been used to address this concept [12]-[14], often just for the particular case of two-port networks with independent terminations.

Here, we consider a quite different scenario. The passivity of the physical structure is granted. It is the predictive model that may be non-passive, due to numerical approximations or measurement errors in its derivation. As such, the model may be useless and may be the root cause for a catastrophic interruption of the design flow. The symptom of this situation is an exponential blow up or a lack of convergence of a transient SPICE run. This work wants to provide some insight in this loss of model stability.

We present an algorithmic procedure that, given a non-passive macromodel, computes a passive termination, with minimal size and dynamic order, that drives the macromodel to instability. This is done regardless of how small the passivity violation is. For the sake of completeness, the developments are carried out down to the synthesis of the destabilizing loads in terms of standard circuit elements (resistors, capacitors, inductors, transformers, and gyrators whenever reciprocity is violated).

A systematic investigation is performed on several classes of structured terminations, with different levels of coupling between the ports. For each of these cases, the conditions allowing for stability loss are explicitly provided. We perform this study since such uncoupled termination schemes are very common in practical designs. Therefore, one might accept a non-passive macromodel provided that it is guaranteed to remain unconditionally stable under uncoupled terminations. We also report the comprehensive set of conditions that guarantee stability for each of the investigated reduced-coupling termination schemes.

Some of the material in this work is not new, since many concepts are borrowed from the field of robust control theory, where the main results were derived some twenty years ago (see, e.g., [22] and references therein). We reinterpret such results in a systematic way to demonstrate that

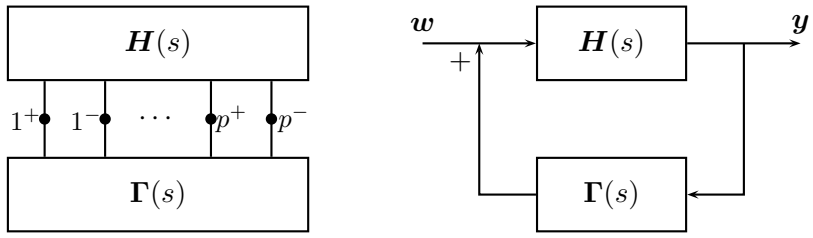

Figure 1: Left: macromodel $\boldsymbol{H}(s)$ with p ports (positive and negative port terminals are denoted with $^+$ and $^-$, respectively) and its termination network $\boldsymbol{\Gamma}(s)$. Right: reformulation of the structure as a feedback loop. Vector $\boldsymbol{y}$ collects output scattering waves at the macromodel ports. Vector $\boldsymbol{w}$ is a disturbance signal entering the feedback loop as an input scattering wave at the macromodel ports. This disturbance represents numerical approximation errors arising in the transient simulation of the entire circuit.

macromodel passivity cannot be ignored and must be taken care of. The material is deliberately presented in a form of a tutorial, working from simplest uncoupled cases (Section 3) to the most general fully-coupled case (Section 4). Section 5 presents a summary of relaxed structure-dependent passivity conditions, while numerical examples are presented in Section 6.

2 Formulation

We consider the situation depicted in the left panel of Fig. 1. No special assumptions on the structure of this macromodel are made to allow for both rational (lumped) and delay-based (transmission-line) macromodels. The p macromodel ports are connected to an unknown termination network $\boldsymbol{\Gamma}(s)$. Throughout this work we will consider both $\boldsymbol{H}(s)$ and $\boldsymbol{\Gamma}(s)$ to be scattering matrices normalized to a common resistance R_0, although a similar derivation can be obtained for other representations. Note that tabulated port responses coming from direct measurements are usually in scattering form, and most full-wave solvers can export their results in scattering form. Therefore, this representation seems to be natural for high-speed interconnect modeling applications.

The macromodel $\boldsymbol{H}(s)$ is considered to be strictly causal and stable, with all poles having negative real part. Causality and stability enforcement is not a critical issue during the identification of the macromodel, since explicit techniques are available for this task [3, 4]. However, we assume that there is at least one frequency band (ω_1, ω_2) where the macromodel exploits a non-passive behavior. For the adopted scattering representation this is equivalent to

$$||\boldsymbol{H}(j\omega)|| > 1, \quad \forall \omega \in (\omega_1, \omega_2)\,, \tag{1}$$

where the euclidean 2-norm is used

$$||\boldsymbol{H}|| = \sigma_{\max}\{\boldsymbol{H}\} = \sqrt{\lambda_{\max}\{\boldsymbol{H}^H\boldsymbol{H}\}}\,, \tag{2}$$

with ^{H} denoting the complex conjugate transpose. In (2), $\sigma_{\max}\{\cdot\}$ and $\lambda_{\max}\{\cdot\}$ denote the maximum singular value and the maximum eigenvalue of their matrix argument, respectively. This norm will be used throughout this work unless otherwise stated. The non-passive frequency bands in (1) can be easily identified, e.g., by using the algorithms proposed in [41] for lumped macromodels and [26] for delay-based macromodels.

We are interested here in the stability properties of the complete circuit as depicted in the left panel of Fig. 1, including the effect of a termination $\boldsymbol{\Gamma}(s)$. This is a standard problem in control theory, since the connection between two multiport elements can be represented as a feedback loop (right panel in Fig. 1). The viewpoint of control theory is to design the termination network such that the feedback structure is well defined and internally stable. Conversely, our interest here is to show how a passive termination network can be designed such that the feedback structure is *not stable*. We will show that this is always possible under the assumption (1) with a fully-coupled p-port termination network. In addition, we will derive the conditions allowing for the synthesis of various destabilizing terminations characterized by less port coupling or no coupling at all. The results will provide quantitative evidence that use of non-passive macromodels should be carefully avoided, and that passivity should be either imposed a priori or enforced using some correction scheme once some passivity violation has been detected.

From Fig. 1 we can easily derive the transfer matrix between a disturbance signal $\boldsymbol{w}(s)$ and the output signal $\boldsymbol{y}(s)$

$$\boldsymbol{y}(s) = \left(\boldsymbol{I} - \boldsymbol{H}(s)\boldsymbol{\Gamma}(s)\right)^{-1}\boldsymbol{H}(s)\boldsymbol{w}(s)\,. \tag{3}$$

The signal $\boldsymbol{w}$ may represent the inevitable numerical errors occurring during a transient simulation of the entire terminated circuit. Instability occurs when this transfer matrix is singular in the right hand plane,

$$\det\{\boldsymbol{I} - \boldsymbol{H}(s_0)\boldsymbol{\Gamma}(s_0)\} = 0\,, \quad \Re\{s_0\} > 0\,. \tag{4}$$

The point s_0 corresponds to an unstable pole of the terminated circuit and gives rise to an exponentially unstable mode $e^{s_0 t}$ in the transient solution. Our main goal is to find both the unstable pole location s_0 and a corresponding passive termination network with scattering matrix $\boldsymbol{\Gamma}(s)$ such that condition (4) is satisfied. In addition, the synthesis of an equivalent circuit for $\boldsymbol{\Gamma}(s)$ will be performed, using only standard circuit elements (resistors, capacitors, inductors, transformers, and gyrators).

The determination of a passive destabilizing termination $\boldsymbol{\Gamma}(s)$ satisfying (4) is simplified by the following fact, proved in [22]

Lemma 1 *Given a complex s_0 with $\Re\{s_0\} > 0$ and a constant matrix $\boldsymbol{\Gamma}_0 \in \mathbb{C}^{p\times p}$, with $||\boldsymbol{\Gamma}_0|| < 1$, it is always possible to find $\boldsymbol{\Gamma}(s)$ regular for $\Re\{s\} \geq 0$ (stable) such that $\boldsymbol{\Gamma}(s_0) = \boldsymbol{\Gamma}_0$ and $||\boldsymbol{\Gamma}(s)|| \leq 1$ for $\Re\{s\} \geq 0$ (passive).*

The above lemma allows us to first look for a constant matrix $\boldsymbol{\Gamma}_0$ such that $\det\{\boldsymbol{I}-\boldsymbol{H}(s_0)\boldsymbol{\Gamma}_0\} = 0$ for some s_0 in the open right plane. The extension of $\boldsymbol{\Gamma}_0$ to the destabilizing termination $\boldsymbol{\Gamma}(s)$ will come for free as an application of Lemma 1.

2.1 Preliminaries: the structured singular value

One of the objectives of this work is to demonstrate the loss of stability under realistic termination schemes as typically found in real high-speed interconnect modeling and simulation. In fact, the general construction of a destabilizing termination available in [22] leads to a load $\boldsymbol{\Gamma}(s)$ that couples all p ports. This situation occurs quite rarely in practical high-speed interconnect simulations, since the near-end and the far-end ports of any interconnect are usually not directly coupled by a common termination network. Therefore, we will investigate here simpler termination structures with less coupling or no coupling at all, highlighting for each case both the conditions leading to instability and providing a synthesis procedure for a corresponding destabilizing termination. The various cases will be analyzed in Sections 3–4.

We report here some preliminary definitions that will be necessary for the study of the terminations with reduced coupling. Technical details are available in [22]. The general structure of the coupling scheme is best represented by a generic constant block-diagonal matrix

$$\boldsymbol{\Delta} = \mathrm{diag}(\boldsymbol{\Delta}_j)\,, \tag{5}$$

where each block of dimension r_j can either be full, $\boldsymbol{\Delta}_j \in \mathbb{C}^{r_j\times r_j}$, or repeated scalar, $\boldsymbol{\Delta}_j = \delta_j \boldsymbol{I}_{r_j}$ with $\delta_j \in \mathbb{C}$. Once the coupling structure is fixed, we are interested in finding both s_0 in the right-hand plane and a corresponding matrix $\boldsymbol{\Delta}_0$ with structure (5) such that

$$\det(\boldsymbol{I} - \boldsymbol{H}(s_0)\boldsymbol{\Delta}_0) = 0\,, \quad \text{and} \quad ||\boldsymbol{\Delta}_0|| < 1\,. \tag{6}$$

The feasibility of this problem is not guaranteed, since specific conditions must hold depending on the particular structure (5). These conditions will be derived in the following. Note that the unitary boundedness of the desired solution $\boldsymbol{\Delta}_0$ is necessary in order to guarantee the passivity of the destabilizing termination to be constructed based on Lemma 1. These considerations lead naturally to adopt the *structured singular value* as a key parameter. This is defined, for a given constant matrix $\boldsymbol{M}$, as

$$\mu_{\boldsymbol{\Delta}}(\boldsymbol{M}) = \frac{1}{\min\{||\boldsymbol{\Delta}||,\, \det(\boldsymbol{I} - \boldsymbol{M}\boldsymbol{\Delta}) = 0\}}\,, \tag{7}$$

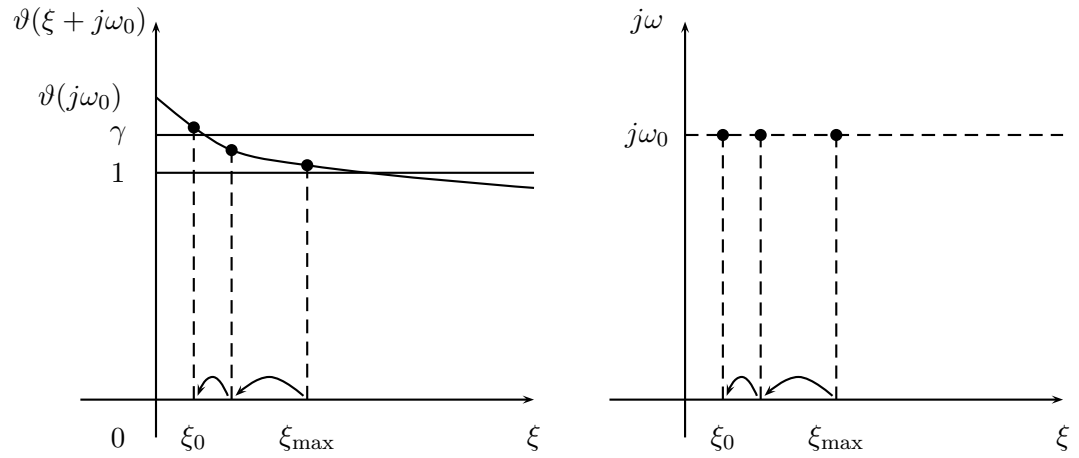

Figure 2: Iterative placement of an unstable pole via Algorithm 1. The left panel reports the value of $\vartheta(\xi + j\omega_0)$ at successive iterations starting from $\xi = \xi_{\max}$. Iterations stop when $\vartheta(\xi + j\omega_0) > \gamma$. Right panel shows the evolution of the unstable pole location in the complex plane through the iterations.

where the minimum is taken over all complex matrices having the prescribed structure (5). This parameter plays a central role in robust control application as well as in present work, since it can be proved [22] that when $\mu_{\boldsymbol{\Delta}}(\boldsymbol{H}(j\omega)) \leq 1$ for all ω, there cannot be a solution to (6). Conversely, such a solution can be found when $\mu_{\boldsymbol{\Delta}}(\boldsymbol{H}(j\omega))$ exceeds one at some frequency ω_0.

Unfortunately, there is no efficient algorithm for the evaluation of the structured singular value (7). However, it is possible to estimate a lower bound, since

$$\max_i |\lambda_i(\boldsymbol{U}\boldsymbol{M})| \leq \mu_{\boldsymbol{\Delta}}(\boldsymbol{M}), \quad \boldsymbol{U}^H\boldsymbol{U} = \boldsymbol{I}, \tag{8}$$

with $\boldsymbol{U}$ sharing the same block-structure of $\boldsymbol{\Delta}$ as in (5), and where $\lambda_i(\cdot)$ denotes the i-th eigenvalue of its matrix argument. Also, it is guaranteed that there is one such matrix $\boldsymbol{U}_{\text{opt}}$ such that the bound (8) holds with the equality sign, i.e., the bound is tight. An algorithm returning an estimate of a lower bound using (8) is reported in [24, 23]. This algorithm returns both a constant matrix $\boldsymbol{\Delta}_0$ having the prescribed block structure (5) such that $\det(\boldsymbol{I} - \boldsymbol{M}\boldsymbol{\Delta}_0) = 0$, and the corresponding lower bound

$$\underline{\mu}_{\boldsymbol{\Delta}}(\boldsymbol{M}) = \frac{1}{||\boldsymbol{\Delta}_0||} \leq \mu_{\boldsymbol{\Delta}}(\boldsymbol{M}) \tag{9}$$

for the structured singular value. Both these quantities will be used in the forthcoming sections for the synthesis of destabilizing terminations in the reduced coupling cases.

Algorithm 1 (determination of the unstable pole $s_0 = \xi_0 + j\omega_0$)

Require: a real nonnegative function $\vartheta(s)$, continuous for $\Re\{s\} \geq 0$, and such that $\vartheta(j\omega_0) > \gamma > 1$ with $\omega_0 > 0$.

Require: a positive constant $\xi_{\max}$

set $\xi := \xi_{\max} > 0$
while $\vartheta(\xi + j\omega_0) \leq \gamma$ **do**
    set $\xi := \xi/2$
end while
set $\xi_0 := \xi$

2.2 Placement of unstable poles

As a preliminary step, we present here a procedure for the determination of the unstable pole s_0. This procedure will be common to all synthesis cases that will be analyzed. The basic requirement is the availability of a real nonnegative function $\vartheta(s)$, continuous for $\Re\{s\} \geq 0$, such that

$$\exists \gamma > 1 : \quad \vartheta(j\omega_0) > \gamma\,, \quad \text{with} \quad \omega_0 > 0\,. \tag{10}$$

As an example, for the fully-coupled synthesis depicted in the left panel of Fig. 1 (to be discussed in Section 4.1), we can assume $\vartheta(s) = ||\boldsymbol{H}(s)||$, so that condition (10) is guaranteed by the assumed passivity violation (1) for the macromodel. Other choices for $\vartheta(s)$ will be detailed in Sections 3–4.

The determination of the unstable pole location can be performed using Algorithm 1 with a suitable choice of $\vartheta(s)$. The algorithm will find

$$s_0 = \xi_0 + j\omega_0 \quad \text{such that} \quad 0 < \xi_0 \leq \xi_{\max} \quad \text{and} \quad \vartheta(s_0) > \gamma > 1\,. \tag{11}$$

A graphical illustration of this procedure is provided in Fig. 2. Termination in a finite (usually small) number of iterations is guaranteed by the continuity condition on $\vartheta(s)$. Guidelines on how to choose the initial value $\xi_{\max}$ will be provided below.

3 Uncoupled termination schemes

We begin the investigation of possible termination schemes driving the macromodel to instability from the simplest cases in which each port is terminated independently. No couplings between any ports are considered in this section. We remark that this type of synthesis is not always possible given a non-passive macromodel $\boldsymbol{H}(s)$. However, we will explicitly provide the conditions that need to be checked in order to insure the feasibility of this synthesis.

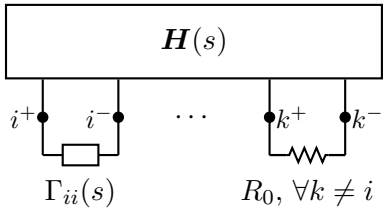

Figure 3: Single-port mismatched termination.

3.1 Single-port mismatched termination

The simplest situation allowing for the design of a destabilizing termination occurs when one of the diagonal elements of scattering matrix $\boldsymbol{H}(s)$ has a magnitude larger than one on the imaginary axis, i.e.,

$$\exists \omega_0 \, \exists \gamma : \, |H_{ii}(j\omega_0)| > \gamma > 1 \, . \tag{12}$$

This condition allows to exploit a single-port resonance by a suitable mismatched one-port termination, as depicted in Fig. 3. All other ports can be matched into the reference resistance R_0, since their contribution is unnecessary. As a result, the scattering matrix $\boldsymbol{\Gamma}(s)$ of the global termination network can be assumed identically vanishing except the diagonal element $\Gamma_{ii}(s)$. It turns out that

$$\det\{\boldsymbol{I} - \boldsymbol{H}(s)\boldsymbol{\Gamma}(s)\} = 1 - H_{ii}(s)\Gamma_{ii}(s) \, , \tag{13}$$

so that the destabilization problem reduces to a scalar synthesis. The singularity condition (4) becomes, by taking magnitude and phase of (13),

$$|H_{ii}(s_0)| \, |\Gamma_{ii}(s_0)| = 1 \, , \quad \angle H_{ii}(s_0) + \angle \Gamma_{ii}(s_0) = 0 \, , \quad \Re\{s_0\} > 0 \, . \tag{14}$$

Since a resistive termination would not be sufficient to fulfill the above condition on the phase, $\Gamma_{ii}(s)$ need to be dynamic. Among the many possible solutions, we assume the following functional form for the reflection coefficient

$$\Gamma_{ii}(s) = \rho \, \frac{\beta - s}{\beta + s} \, , \quad -1 \leq \rho \leq 1 \, , \quad \beta \geq 0 \, , \quad \beta < \infty \, . \tag{15}$$

This corresponds to a two-parameter family of first-order terminations, which can be synthesized as in Table 1. Note that the bounds on ρ and β insure that this load is stable and passive. We remark that alternative solutions of (14) with arbitrary dynamic order are indeed possible but are not investigated here.

The feasibility of this choice is guaranteed, since

$$\xi_0 \leq \xi_{\max} = \omega_0 \frac{\gamma^2 - 1}{2\gamma} \quad \Leftrightarrow \quad \sqrt{\frac{(\xi_0 - \beta)^2 + \omega_0^2}{(\xi_0 + \beta)^2 + \omega_0^2}} \geq \frac{1}{\gamma} \, , \quad \forall \beta \geq 0 \, , \tag{16}$$

as can be proved via a straightforward calculation. This condition implies that it is possible to determine ρ such that the magnitude condition in (14) is satisfied with $|\rho| \leq 1$, independent of

β. The actual identification of the two unknown parameters ρ and β is performed by following the few steps below.

1. First, we set $\vartheta(s) = |H_{ii}(s)|$ and we use Algorithm 1 with $\xi_{\max}$ defined as in (16) to identify the real part $\xi_0 > 0$ of what will be an unstable pole $s_0 = \xi_0 + j\omega_0$ of the terminated circuit. Note that the algorithm insures that $|H_{ii}(\xi_0 + j\omega_0)| > \gamma > 1$.

2. Once ξ_0 is known, the phase condition in (14) can be satisfied by finding β such that

$$\phi(\beta) = \pi - \angle H_{ii}(\xi_0 + j\omega_0) - \angle\rho\,, \tag{17}$$

   where

$$\angle\rho = \begin{cases} 0, & \text{if} \quad \angle H_{ii}(\xi_0 + j\omega_0) \in (0, \pi) \\ \pi, & \text{if} \quad \angle H_{ii}(\xi_0 + j\omega_0) \in (-\pi, 0) \end{cases} \tag{18}$$

   and

$$\phi(\beta) = \arctan\frac{\beta - \xi_0}{\omega_0} + \arctan\frac{\beta + \xi_0}{\omega_0} \tag{19}$$

   Since $\phi(\beta)$ is regular and monotonically increasing from 0 to π as β increases from 0 to ∞, the solution to (17) is unique and is easily found, e.g., by few Newton-Raphson iterations.

3. Finally, the magnitude condition is satisfied by choosing

$$|\rho| = \frac{1}{|H_{ii}(\xi_0 + j\omega_0)|}\sqrt{\frac{(\xi_0 + \beta)^2 + \omega_0^2}{(\xi_0 - \beta)^2 + \omega_0^2}}\,, \tag{20}$$

   which is bounded by one due to (12) and (16). Hence, passivity of $\Gamma_{ii}(s)$ is guaranteed.

4. The particular case of purely real $H_{ii}(\xi_0 + j\omega_0)$ is handled by choosing $\beta = 0$ and $\rho = 1/H_{ii}(\xi_0 + j\omega_0)$.

Whenever one of the diagonal entries of the macromodel scattering matrix is larger than one, the above procedure leads to a passive scalar first-order load defined in (15). This load is easily synthesized into an equivalent circuit as summarized in Table 1 for all various combinations of the parameters.

A few remarks on the constant γ. This constant is used to parameterize the design, in the following sense. When γ tends to one from above, the real part of the resulting pole s_0 is the largest possible (see Algorithm 1), thus leading to faster exponential blow up of the terminated circuit. In such case, the termination becomes close to lossless, see (14) and Table 1. Larger values of γ allow for more dissipative destabilizing loads but lead to unstable poles that are very close to the imaginary axis, corresponding to a slower exponential blow up rate of the terminated circuit.

Table 1: Synthesis of a scalar first-order load (15) with $\beta \geq 0$ and $|\rho| \leq 1$

ρ	β	Circuit	Elements
0	$\forall$	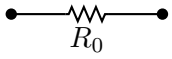	
1	0		
-1	0		
$\lvert\cdot\rvert < 1$	0		$R = R_0 \frac{1-\rho}{1+\rho}$
1	> 0	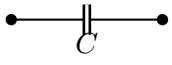	$C = \frac{1}{\beta R_0}$
-1	> 0	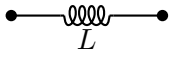	$L = \frac{R_0}{\beta}$
> 0	> 0	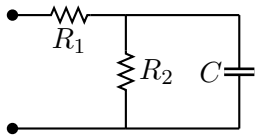	$R_1 = R_0 \frac{1-\rho}{1+\rho}$ $R_2 = R_0 \frac{4\rho}{1-\rho^2}$ $C = \frac{(1+\rho)^2}{4\rho\beta R_0}$
< 0	> 0	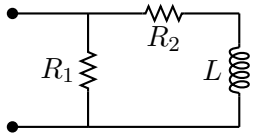	$R_1 = R_0 \frac{1-\rho}{1+\rho}$ $R_2 = R_0 \frac{1-\rho^2}{-4\rho}$ $L = \frac{R_0(1-\rho)^2}{-4\rho\beta}$

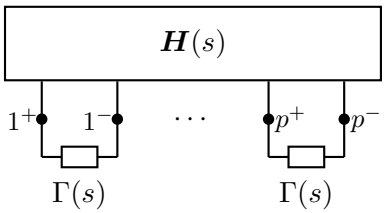

Figure 4: Identical scalar terminations.

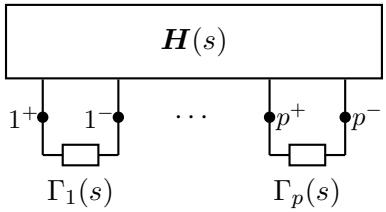

Figure 5: Scalar terminations.

3.2 Identical scalar terminations

Another load structure that reduces to a scalar synthesis is a set of identical uncoupled scalar terminations, depicted in Fig. 4. The corresponding scattering matrix is diagonal with identical entries,

$$\boldsymbol{\Gamma}(s) = \Gamma(s)\boldsymbol{I}\,. \tag{21}$$

In fact, using the eigendecomposition $\boldsymbol{H}(s) = \boldsymbol{V}^{-1}(s)\mathrm{diag}\{\lambda_i(s)\}\boldsymbol{V}(s)$, we obtain

$$\det\{\boldsymbol{I} - \boldsymbol{H}(s)\boldsymbol{\Gamma}(s)\} = \prod_i (1 - \lambda_i(s)\Gamma(s))\,. \tag{22}$$

Loss of stability occurs when any term in the above product vanishes at any s_0 with $\Re\{s_0\} > 0$. This is guaranteed by the condition

$$\exists\omega_0\,\exists\gamma:\ \max_i |\lambda_i(\boldsymbol{H}(j\omega_0))| > \gamma > 1\,, \tag{23}$$

which can be easily checked by a sweep within the frequency bands (1) where the macromodel exploits a non-passive behavior. If ω_0 satisfying (23) is found, the same procedure of section 3.1 can be used with only slight modifications. The only differences are

- the use of $\vartheta(s) = \max_i |\lambda_i(\boldsymbol{H}(s))|$ in Algorithm 1 for the identification of the unstable pole location;
- use of $\lambda_i(\boldsymbol{H}(\xi + j\omega_0)$ instead of $H_{ii}(\xi + j\omega_0)$ in steps 2 and 3 for the determination of ρ and β defining $\Gamma(s)$ as in (15).

The corresponding equivalent circuit for $\Gamma(s)$ can be synthesized according to Table 1. The above derivation insures that termination of each macromodel port as in Fig. 4 leads to instability the system.

3.3 Scalar terminations

The next level of complexity is obtained by releasing the constraint of identical loads and keeping the constraint of independent uncoupled terminations, as depicted in Fig. 5. The corresponding

scattering matrix is diagonal

$$\boldsymbol{\Gamma}(s) = \mathrm{diag}\{\Gamma_i(s)\}\,. \tag{24}$$

Theorem 11.8 in [22] states that a necessary and sufficient condition for the loss of stability of the system with passive $\Gamma_i(s)$ is

$$\exists\omega_0\,\exists\gamma:\ \mu_{\boldsymbol{\Delta}}(\boldsymbol{H}(j\omega_0)) > \gamma > 1\,,\quad \boldsymbol{\Delta} = \mathrm{diag}(\delta_i)\,,\quad \delta_i \in \mathbb{C}\,, \tag{25}$$

where the structured singular value (7) corresponding to a diagonal block structure is used. As introduced in Section 2.1, the computation of μ is difficult. Therefore, we will use the condition

$$\exists\omega_0\,\exists\gamma:\ \underline{\mu}_{\boldsymbol{\Delta}}(\boldsymbol{H}(j\omega_0)) > \gamma > 1\,,\quad \boldsymbol{\Delta} = \mathrm{diag}(\delta_i)\,,\quad \delta_i \in \mathbb{C}\,, \tag{26}$$

where the lower bound (9) is used instead of the actual structured singular value. Condition (26) can be easily checked by a search within the frequency bands where $\boldsymbol{H}(s)$ exploits a non-passive behavior. When this condition is satisfied, we can use $\vartheta(s) = \underline{\mu}_{\boldsymbol{\Delta}}(\boldsymbol{H}(s))$ in Algorithm 1 to identify the location s_0 of the unstable pole. As a byproduct from the lower bound computation, we obtain $\underline{\mu}_0 = \underline{\mu}_{\boldsymbol{\Delta}}(\boldsymbol{H}(s_0))$ and a constant complex matrix $\boldsymbol{\Gamma}_0 = \mathrm{diag}\{\Gamma_{i,0}\}$ such that

$$\det(\boldsymbol{I} - \boldsymbol{H}(s_0)\boldsymbol{\Gamma}_0) = 0 \quad \text{and} \quad ||\boldsymbol{\Gamma}_0|| = \max_i |\Gamma_{i,0}| = 1/\underline{\mu}_0 < 1\,. \tag{27}$$

Since diagonal structure is assumed here, the synthesis of each independent load is achieved by computing $\beta_i \geq 0$ and ρ_i with $|\rho_i| \leq 1$ such that

$$\rho_i\,\frac{\beta_i - s_0}{\beta_i + s_0} = \Gamma_{i,0}\,. \tag{28}$$

This problem has already been solved in Sec. 3.1, with the circuit synthesis reported in Table 1. As a result, we obtain a set of p independent first-order scalar loads providing a destabilizing termination network for the macromodel according to Fig. 5.

As a final remark, we note that when no ω_0 and γ can be found to fulfill condition (25), the macromodel is guaranteed to remain stable regardless of its (passive) port terminations, as far as they are uncoupled.

4 Coupled termination schemes

The destabilization of a non-passive macromodel is always possible, at least with a fully coupled termination $\boldsymbol{\Gamma}(s)$. We will detail in Sections 4.1 and 4.2 the construction and the circuit synthesis of such a termination. However, we will detail in Section 4.3 another termination scheme made of two uncoupled blocks, which is very often encountered for transmission line and interconnect structures.

4.1 Fully coupled termination

The termination structures discussed in Section 3 may not always be applicable in the general case. However, a destabilizing termination network can always be found by leaving all couplings, as depicted in the left panel of Fig. 1, since the condition

$$\exists \omega_0 \, \exists \gamma : \, ||\boldsymbol{H}(j\omega_0)|| > \gamma > 1 \tag{29}$$

is guaranteed by working assumption (1) of a non-passive macromodel $\boldsymbol{H}(s)$. The localization of the unstable pole is achieved using $\vartheta(s) = ||\boldsymbol{H}(s)||$ in Algorithm 1. In this fully coupled case, a slightly more stringent initialization of ξ is also needed in Algorithm 1 (line 3) with respect to the scalar case (16). More precisely, we set

$$\xi_{\max} := \omega_0 \frac{\gamma - 1}{2\sqrt{\gamma}} \tag{30}$$

This condition guarantees that the unstable pole $s_0 = \xi_0 + j\omega_0$ will have a real part ξ_0 such that

$$\sqrt{\frac{(\xi_0 + \beta)^2 + \omega_0^2}{(\xi_0 - \beta)^2 + \omega_0^2}} \leq \sqrt{\gamma} \,, \quad \forall \beta \geq 0 \,, \tag{31}$$

as can be easily verified by a straightforward calculation.

A procedure for the construction of $\boldsymbol{\Gamma}(s)$ can be found in [22]. We report here the main steps for completeness. We start noting that in correspondence of s_0 we have $\sigma_1 = ||\boldsymbol{H}(s_0)|| > \gamma > 1$. We compute the singular value decomposition of this (constant complex) matrix, as

$$\boldsymbol{H}(s_0) = \boldsymbol{U} \mathrm{diag}\{\sigma_i\} \boldsymbol{V}^H \,. \tag{32}$$

Next, we define

$$\boldsymbol{\Gamma}_0 = \frac{1}{\sigma_1} \boldsymbol{v}_1 \boldsymbol{u}_1^H \,, \tag{33}$$

where σ_1 is the largest (first) singular value and $\boldsymbol{v}_1$, $\boldsymbol{u}_1$ are the corresponding right and left singular vectors (first columns of $\boldsymbol{V}$ and $\boldsymbol{U}$, respectively). Note that $||\Gamma_0|| = 1/\sigma_1 < 1$ by construction. We have

$$\begin{aligned}
\det\{\boldsymbol{I} - \boldsymbol{H}(s_0)\boldsymbol{\Gamma}_0\} &= \det\left\{\boldsymbol{I} - \boldsymbol{U}\mathrm{diag}\{\sigma_i\}\boldsymbol{V}^H \frac{1}{\sigma_1}\boldsymbol{v}_1\boldsymbol{u}_1^H\right\} \\
&= \det\left\{\boldsymbol{U}\left(\boldsymbol{I} - \mathrm{diag}\left\{\frac{\sigma_i}{\sigma_1}\right\}\boldsymbol{V}^H\boldsymbol{v}_1\boldsymbol{u}_1^H\boldsymbol{U}\right)\boldsymbol{U}^H\right\} \\
&= \det\left\{\boldsymbol{U}\left(\boldsymbol{I} - \mathrm{diag}\left\{\frac{\sigma_i}{\sigma_1}\right\}(1\,0\,\ldots\,0)^T(1\,0\,\ldots\,0)\right)\boldsymbol{U}^H\right\} \\
&= \det\{\boldsymbol{U}\mathrm{diag}\{0,1,\ldots,1\}\boldsymbol{U}^H\} = 0 \,,
\end{aligned}$$

so that the singularity condition (4) at s_0 is satisfied for any termination $\boldsymbol{\Gamma}(s)$ such that $\boldsymbol{\Gamma}(s_0) = \boldsymbol{\Gamma}_0$. The existence of such termination (which has to be stable and passive) is guaranteed by

Lemma 1. The actual construction is achieved by finding $\rho_{1,i}$, $\rho_{2,i}$, $\beta_{1,i}$, $\beta_{2,i}$ for each component of the singular vectors $\boldsymbol{v}_1$ and $\boldsymbol{u}_1$, such that

$$\rho_{1,i}\,\frac{\beta_{1,i}-s_0}{\beta_{1,i}+s_0}=\frac{v_{1,i}}{\sqrt{\sigma_1}}\,,\quad \rho_{2,i}\,\frac{\beta_{2,i}-s_0}{\beta_{2,i}+s_0}=\frac{u^*_{1,i}}{\sqrt{\sigma_1}}\,,\quad \beta_{1,i},\beta_{2,i}\geq 0\,,\quad -1\leq\rho_{1,i},\rho_{2,i}\leq 1\,. \tag{34}$$

The problem is thus reduced to $2p$ independent constructions, which have already been dealt with in Section 3.1 (see Eqs. 14 and 15). Assembling all components, we obtain a stable and fully coupled destabilizing termination as

$$\boldsymbol{\Gamma}(s)=\boldsymbol{\rho}_1(s)\boldsymbol{\rho}_2^T(s)\,,\quad (\boldsymbol{\rho}_1(s))_i=\rho_{1,i}\,\frac{\beta_{1,i}-s}{\beta_{1,i}+s}\,,\quad (\boldsymbol{\rho}_2(s))_i=\rho_{2,i}\,\frac{\beta_{2,i}-s}{\beta_{2,i}+s} \tag{35}$$

It turns out that this definition insures also passivity. In fact, using the definition (34), we can see that each component of these two vectors is bounded as

$$|(\boldsymbol{\rho}_1(s))_i|\leq|\rho_{1,i}|\leq\sqrt{\frac{(\xi_0+\beta)^2+\omega_0^2}{(\xi_0-\beta)^2+\omega_0^2}}\,\frac{|v_{1,i}|}{\sqrt{\sigma_1}}<|v_{1,i}| \tag{36}$$

due to (31), and similarly for $\boldsymbol{\rho}_2(s)$. Since $\boldsymbol{\Gamma}(s)$ is a rank-one scattering matrix for each value of the complex frequency s, its maximum singular value is easily computed as

$$||\boldsymbol{\Gamma}(s)||=||\boldsymbol{\rho}_1(s)||\,||\boldsymbol{\rho}_2(s)||<||\boldsymbol{v}_1||\,||\boldsymbol{u}_1||=1 \tag{37}$$

due to the orthonormality of the right and left singular vectors. The above bound proves passivity of $\boldsymbol{\Gamma}(s)$.

4.2 Circuit synthesis for the fully coupled case

We provide here a possible circuit synthesis for the fully coupled termination with scattering matrix (35). The latter can be restated as a factorization into three matrix terms,

$$\boldsymbol{\Gamma}(s)=\boldsymbol{\Gamma}'(s)\,\boldsymbol{\Gamma}_{DC}\,\boldsymbol{\Gamma}''(s) \tag{38}$$

where

$$\boldsymbol{\Gamma}_{DC}=\boldsymbol{r}_1\boldsymbol{r}_2^T\,,\quad \text{with}\quad r_{k,i}=\rho_{k,i}\,,\quad k=1,2\,,\quad i=1,\ldots,p \tag{39}$$

denotes $\boldsymbol{\Gamma}(s=0)$, and where

$$\boldsymbol{\Gamma}'(s)=\mathrm{diag}\left\{\frac{\beta_{1,i}-s}{\beta_{1,i}+s}\right\}=\mathrm{diag}\{\Gamma'_i(s)\}\,,\quad \boldsymbol{\Gamma}''(s)=\mathrm{diag}\left\{\frac{\beta_{2,i}-s}{\beta_{2,i}+s}\right\}=\mathrm{diag}\{\Gamma''_i(s)\} \tag{40}$$

are diagonal and para-unitary. Equivalently, $\boldsymbol{\Gamma}'(s)$ and $\boldsymbol{\Gamma}''(s)$ are the scattering matrices of two lossless and fully uncoupled multiports, with each diagonal entry representing the reflection coefficient of a single capacitance $C'_i=1/(\beta_{1,i}R_0)$ or $C''_i=1/(\beta_{2,i}R_0)$, as depicted in Table 1.

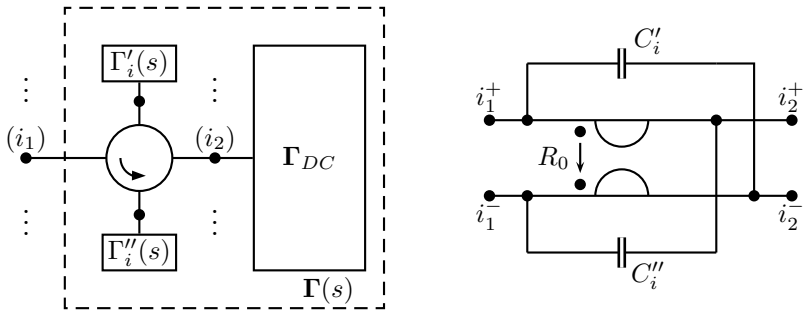

Figure 6: Left: Realization of $\mathbf{\Gamma}(s)$ in (38) via a 4-port circulator connected to each port (i_2) of $\mathbf{\Gamma}_{DC}$ and loaded by two reflection coefficients $\Gamma_i'(s)$ and $\Gamma_i''(s)$. Right: circuit implementation of the loaded circulator section (superscripts $^+$ and $^-$ denote positive and negative terminals of each port, respectively). See also text.

The circuit synthesis of the product (38) can be performed using circulators. The basic block structure depicted in Fig. 6 (left panel) is readily shown by a signal flow analysis to be equivalent to (38). In fact, an incident wave into port (i_1) of $\mathbf{\Gamma}(s)$ is redirected into $\Gamma_i''(s)$, which reflects it into the port (i_2) of $\mathbf{\Gamma}_{DC}$. The corresponding reflected wave is redirected into $\Gamma_i'(s)$, which finally reflects it at the output. The actual circuit implementation of the loaded circulator section, i.e., the two-port connected between ports (i_1) and (i_2), is available in the right panel of Fig. 6. This two-port has a scattering matrix of the form

$$\boldsymbol{S}_i(s) = \begin{pmatrix} 0 & \Gamma_i'(s) \\ \Gamma_i''(s) & 0 \end{pmatrix} \tag{41}$$

Note that the gyrator cannot be avoided since the construction of $\Gamma_i'(s)$ and $\Gamma_i''(s)$ is independent, implying $\beta_{1,i} \neq \beta_{2,i}$ in the general case.

The gyrator can be eliminated when the macromodel under investigation is reciprocal, i.e., when its associated scattering matrix $\boldsymbol{H}(s)$ is symmetric. In this case, the matrices $\boldsymbol{U}$ and $\boldsymbol{V}$ in the singular value decomposition (32) of $\boldsymbol{H}(s_0) = \boldsymbol{H}^T(s_0)$ can be shown to be the complex conjugate one of each other up to arbitrary phase terms, i.e.,

$$\boldsymbol{U} = \boldsymbol{V}^* \mathrm{diag}\{e^{j\theta_i}\}\,. \tag{42}$$

A redefinition of the left singular vectors via compensation of these phase terms, i.e., by setting $\theta_i = 0$, leads to the equivalent decomposition

$$\boldsymbol{H}(s_0) = \boldsymbol{V}^* \mathrm{diag}\{\sigma_i\} \boldsymbol{V}^H\,, \tag{43}$$

which explicitly preserves symmetry. This in turns allows to define

$$\mathbf{\Gamma}_0 = \frac{1}{\sigma_1} \boldsymbol{v}_1 \boldsymbol{v}_1^T \tag{44}$$

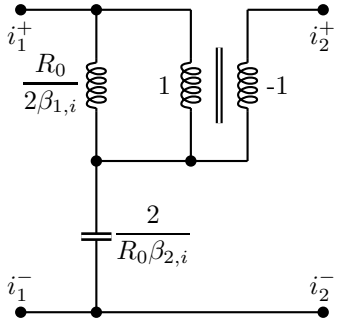

Figure 7: Circuit realization of the loaded circulator section of Fig. 6 in the reciprocal case.

instead of (33), leading to $\rho_{2,i} = \rho_{1,i}$ and $\beta_{2,i} = \beta_{1,i}$ in (34) and (35). Consequently, the two capacitances in the loaded circulator section depicted in Fig. 6 become identical, $C_i'' = C_i'$ and the corresponding scattering matrix (41) becomes symmetric and represents a matched lossless reciprocal all-pass two-port. The circuit synthesis becomes therefore a canonical problem (see [8], p. 215). A possible circuit realization using only one ideal transformer with turns-ratio $(-1:1)$ is illustrated in Fig. 7.

We turn now to the synthesis of the purely resistive multiport $\boldsymbol{\Gamma}_{DC}$. Since all ports are assumed to be referenced to the same resistance R_0, the (constant real) impedance matrix of the multiport is obtained as

$$\boldsymbol{R}_{DC} = R_0(\boldsymbol{I} + \boldsymbol{\Gamma}_{DC})(\boldsymbol{I} - \boldsymbol{\Gamma}_{DC})^{-1}\,, \tag{45}$$

which is always defined and strictly positive definite since $||\boldsymbol{\Gamma}_{DC}|| < 1$ by construction. Using expression (39) we get, after few straightforward algebraic manipulations,

$$\boldsymbol{R}_{DC} = R_0\left(\boldsymbol{I} + \alpha\,\boldsymbol{r}_1\boldsymbol{r}_2^T\right)\,, \quad \alpha = \frac{2}{1 - \boldsymbol{r}_2^T\boldsymbol{r}_1} > 0\,, \tag{46}$$

showing that this DC impedance matrix is a rank-one perturbation of a matched diagonal termination.

This synthesis of $\boldsymbol{R}_{DC}$ is a canonical problem, fully developed in [8]. The impedance matrix is first decomposed into its symmetric and skew-symmetric parts

$$\boldsymbol{R}_{DC} = \boldsymbol{R'} + \boldsymbol{R''}\,, \quad \boldsymbol{R'} = R_0\boldsymbol{I} + R_0\alpha\,(\boldsymbol{r}_1\boldsymbol{r}_2^T + \boldsymbol{r}_2\boldsymbol{r}_1^T)\,, \quad \boldsymbol{R''} = R_0\alpha\,(\boldsymbol{r}_1\boldsymbol{r}_2^T - \boldsymbol{r}_2\boldsymbol{r}_1^T)\,. \tag{47}$$

Thus, $\boldsymbol{R}_{DC}$ is synthesized as a series connection of two p-port networks, which can realized using positive resistors, ideal transformers, and gyrators. More precisely, the symmetric part is transformed via Gauss algorithm as

$$\boldsymbol{R'} = \boldsymbol{N'}^T\boldsymbol{\Lambda'}\boldsymbol{N'}\,, \quad \boldsymbol{\Lambda'} = \mathrm{diag}\{\lambda_i'\} \geq 0\,, \tag{48}$$

which is interpreted as a $2p$-port ideal transformer network having a turns-ratio matrix $\boldsymbol{N'}$. The p shunt ports of this transformer network are closed on positive resistances λ_i'. Similarly, the

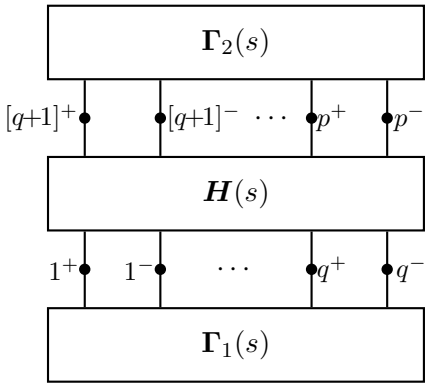

Figure 8: Two-block uncoupled terminations.

skew-symmetric part is reduced as

$$\boldsymbol{R''} = \boldsymbol{N''}^T \boldsymbol{\Lambda''} \boldsymbol{N''}\,, \quad \boldsymbol{\Lambda''} = \begin{pmatrix} 0 & R_0\alpha \\ -R_0\alpha & 0 \end{pmatrix}, \quad \boldsymbol{N''} = \begin{pmatrix} \boldsymbol{r}_2^T \\ \boldsymbol{r}_1^T \end{pmatrix}, \tag{49}$$

which is interpreted as a rank-2 $(p+2)$-port transformer network having turns-ratio matrix $\boldsymbol{N''}$, whose two shunt ports are closed on an ideal gyrator with resistance $R_0\alpha$. Finally, we remark that in the reciprocal case we have $\boldsymbol{r}_1 = \boldsymbol{r}_2$, implying that the synthesis can be performed directly using (46) as a rank-1 $(p+1)$-port transformer network having turns-ratio matrix $\boldsymbol{r}_1^T$, with its shunt port loaded on a resistor $R_0\alpha$, and with resistors R_0 connected in series to each of its series ports.

4.3 Two uncoupled blocks

More general termination schemes can be adopted, other than the fully uncoupled and the fully coupled cases. Many combinations are possible, so we consider here only one case which is the typical setting for high-speed interconnects and transmission-line simulation. Without loss of generality we assume p even and we split the ports into two uncoupled sets of size $q = p/2$, defining a two-block termination structure depicted in Fig. 8. The corresponding scattering matrix is block-diagonal

$$\boldsymbol{\Gamma}(s) = \mathrm{diag}\{\boldsymbol{\Gamma}_1(s), \boldsymbol{\Gamma}_2(s)\}\,. \tag{50}$$

The basic condition allowing for this two-block destabilization is

$$\exists \omega_0 : \mu_{\boldsymbol{\Delta}}(\boldsymbol{H}(j\omega_0)) \geq \underline{\mu}_{\boldsymbol{\Delta}}(\boldsymbol{H}(j\omega_0)) > \gamma > 1\,, \quad \boldsymbol{\Delta} = \mathrm{diag}(\boldsymbol{\Delta}_1, \boldsymbol{\Delta}_2)\,, \quad \boldsymbol{\Delta}_i \in \mathbb{C}^{q,q}\,. \tag{51}$$

Also this condition can be checked by a search within the non-passive bandwidths of the macromodel. When (51) is fulfilled, application of Algorithm 1 with $\vartheta(s) = \underline{\mu}_{\boldsymbol{\Delta}}(\boldsymbol{H}(s))$ and with the initialization (30) leads to the location of the unstable pole $s_0 = \xi_0 + j\omega_0$ and to a pair of constant complex matrices $\boldsymbol{\Gamma}_{0,k}$, $k = 1, 2$ such that

$$\det(\boldsymbol{I} - \boldsymbol{H}(s_0)\boldsymbol{\Gamma}_0) = 0\,, \quad \boldsymbol{\Gamma}_0 = \mathrm{diag}(\boldsymbol{\Gamma}_{0,k}) \quad \text{and} \quad ||\boldsymbol{\Gamma}_{0,k}|| < 1\,. \tag{52}$$

Table 2: Relaxed passivity conditions under structured terminations. If the conditions in the right column are fulfilled, the macromodel with a stable scattering matrix $\boldsymbol{H}(s)$ preserves its stability when terminated by a load with the coupling structure reported in the left column.

Load structure	Structured passivity condition
Single-port mismatch	$\lvert H_{ii}(j\omega)\rvert \leq 1, \quad \forall\omega\,\forall i$
Identical scalar	$\max_i \lvert\lambda_i(\boldsymbol{H}(j\omega))\rvert \leq 1, \quad \forall\omega\,\forall i$
Scalar	$\mu_{\boldsymbol{\Delta}}(\boldsymbol{H}(j\omega)) \leq 1 \quad \forall\omega, \quad \boldsymbol{\Delta} = \mathrm{diag}(\delta_i)\,, \quad \delta_i \in \mathbb{C}$
Two-block	$\mu_{\boldsymbol{\Delta}}(\boldsymbol{H}(j\omega)) \leq 1 \quad \forall\omega, \quad \boldsymbol{\Delta} = \mathrm{diag}(\boldsymbol{\Delta}_1, \boldsymbol{\Delta}_2), \quad \boldsymbol{\Delta}_i \in \mathbb{C}^{q,q}$
Full	$\lVert\boldsymbol{H}(j\omega)\rVert \leq 1, \quad \forall\omega$

This condition guarantees that $\boldsymbol{H}(s_0)\boldsymbol{\Gamma}_0$ has a unitary eigenvalue. Denoting as $\boldsymbol{x}_1$ and $\boldsymbol{x}_2$ the two block components of the corresponding eigenvector, we define

$$\widetilde{\boldsymbol{\Gamma}}_{0,k} = \widetilde{\boldsymbol{v}}_k \widetilde{\boldsymbol{u}}_k^H\,, \quad \text{with} \quad \widetilde{\boldsymbol{v}}_k = \frac{\boldsymbol{\Gamma}_{0,k}\boldsymbol{x}_k}{\lVert\boldsymbol{\Gamma}_{0,k}\rVert^{1/2}\,\lVert\boldsymbol{x}_k\rVert}\,, \quad \widetilde{\boldsymbol{u}}_k = \frac{\boldsymbol{x}_k}{\lVert\boldsymbol{x}_k\rVert}\lVert\boldsymbol{\Gamma}_{0,k}\rVert^{1/2}\,, \tag{53}$$

unless $\boldsymbol{x}_k = 0$, in which case we set $\widetilde{\boldsymbol{\Gamma}}_{0,k} = \boldsymbol{0}$. Clearly, $\lVert\widetilde{\boldsymbol{\Gamma}}_{0,k}\rVert < 1$. This enables the construction of a passive two-block dynamic termination as in (50) such that

$$\boldsymbol{\Gamma}_k(s_0) = \widetilde{\boldsymbol{\Gamma}}_{0,k}\,, \tag{54}$$

using the same procedure already employed for the fully coupled case and detailed in Section 4.1. The result is, for each block $k = 1, 2$

$$\boldsymbol{\Gamma}_k(s) = \boldsymbol{\rho}_1^k(s)(\boldsymbol{\rho}_2^k(s))^T \tag{55}$$

with each component being defined as in (35) for the fully coupled case. Finally, the circuit synthesis can be performed for each independent block following the procedure of Section 4.2.

5 Structure-dependent passivity

The developments of Sections 3 and 4 have been carried out with the intention of demonstrating the loss of stability of a macromodel under various passive termination schemes with different coupling structure. For a quick comparison, a visual summary of all these terminations is depicted in Figure 9. In this short section we change perspective. Indeed, the main theoretical results can be restated in terms of relaxed "structured" passivity conditions, which guarantee macromodel stability when it is terminated by a load having a prescribed coupling structure. These conditions are listed in Table 2 for all cases investigated in this paper.

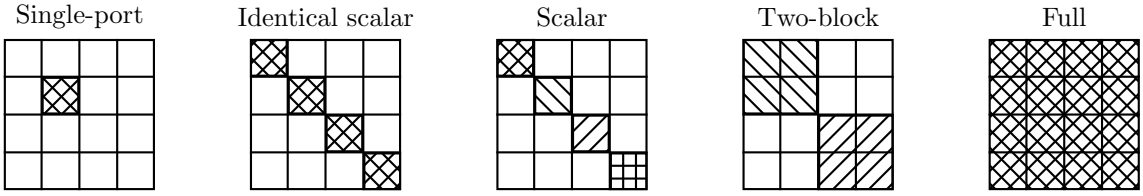

Figure 9: Outline of the scattering matrix $\boldsymbol{\Gamma}(s)$ for all termination schemes presented in the paper, referred to a macromodel $\boldsymbol{H}(s)$ having 4 ports. Only the nonvanishing entries of $\boldsymbol{\Gamma}(s)$ are depicted with filled boxes. Within each panel, different filling schemes denote different independent subcircuits.

Figure 10: Layout of the PCB with the coupled interconnect structure under investigation. Port numbering is also specified.

6 Examples

6.1 Lumped macromodel

We illustrate the destabilization procedure on a practical example. The Printed Circuit Board (PCB) coupled interconnect depicted in Fig. 10 has been characterized by a set of measured Scattering parameters referred to $R_0 = 50\,\Omega$, over a 1 GHz bandwidth. This dataset has been used to compute a rational macromodel via the VF algorithm [3]. This macromodel results non-passive, since a frequency-sweep of the corresponding $||\boldsymbol{H}(j\omega)||$ returns values larger than one. We remark that the physical interconnect structure is certainly passive. Passivity violations are here introduced in the measurement process and are essentially due to an imperfect instrument calibration. Figure 11 reports the norm $||\boldsymbol{H}(j\omega)||$ (curve labeled as "full") and some additional frequency-dependent structured singular values corresponding to the two-block, scalar, and identical scalar termination schemes. All these norms exceed one in three different frequency bands, thus enabling the application of the proposed destabilization scheme.

Three independent sets of passive terminations have been designed for each passivity violation bandwidth, with a prescribed coupling structure. In particular, Algorithm 1 has been executed in each case by choosing the frequency ω_0 that maximizes the norm of interest ("full", "two-block", "scalar", and "identical scalar") within each of the three available frequency bands. Then,

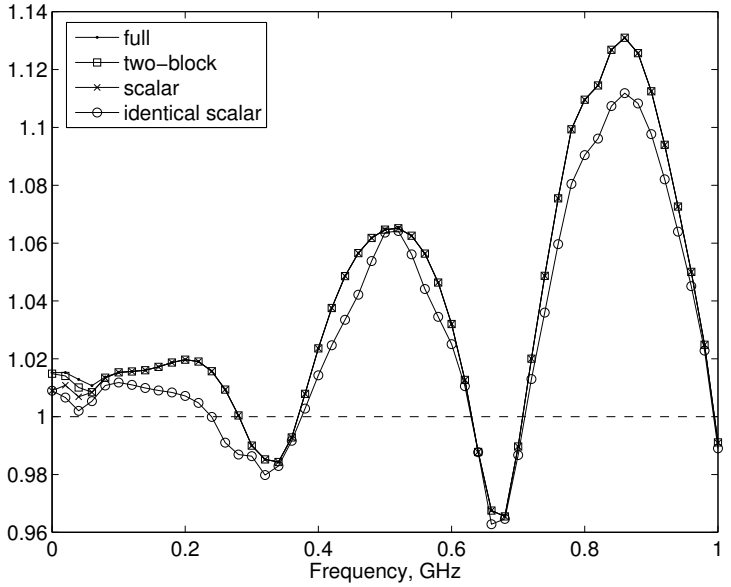

Figure 11: Frequency-dependent structured norms for a non-passive macromodel of a PCB interconnect structure. Three passivity violation bands are visible; band I: $(0, 0.3)$ GHz, band II: $(0.4, 0.6)$ GHz, band III: $(0.7, 1)$ GHz. The "full", "two-block" and "scalar" curves are almost superimposed, except for a small bandwidth at low frequency.

Table 3: Unstable poles for various termination schemes. Each column correspond to a different design based on the location of the target unstable poles in frequency bands I, II, and III, respectively.

Termination scheme	Unstable poles [Grad/s]		
	Band I	Band II	Band III
Fully coupled	$0.0032 \pm j1.3195$	$0.0129 \pm j3.2044$	$0.0430 \pm j5.4350$
Two-block	$0.0032 \pm j1.3195$	$0.0129 \pm j3.2044$	$0.0430 \pm j5.4350$
	$0.0097 \pm j2.8865$	$0.0209 \pm j4.9577$	
Scalar	$0.0032 \pm j1.3195$	$0.0129 \pm j3.2044$	$0.0430 \pm j5.4350$
	$0.0272 \pm j2.8792$	$0.0253 \pm j4.8872$	
	$0.0317 \pm j4.6895$		
Identical scalar	$0.0038 \pm j0.6597$	$0.0128 \pm j3.2044$	$0.0369 \pm j5.4350$
	0.0005	$0.0259 \pm j4.8886$	

the corresponding twelve different de-stabilizing terminations have been computed. Finally, the twelve sets of poles of the complete network (macromodel plus each of the terminations) have been computed. Figure 12 reports the network poles for one of these cases (identical scalar terminations designed within band III) and shows the presence of two unstable poles, as expected. The set of unstable poles for each case is reported in Table 3.

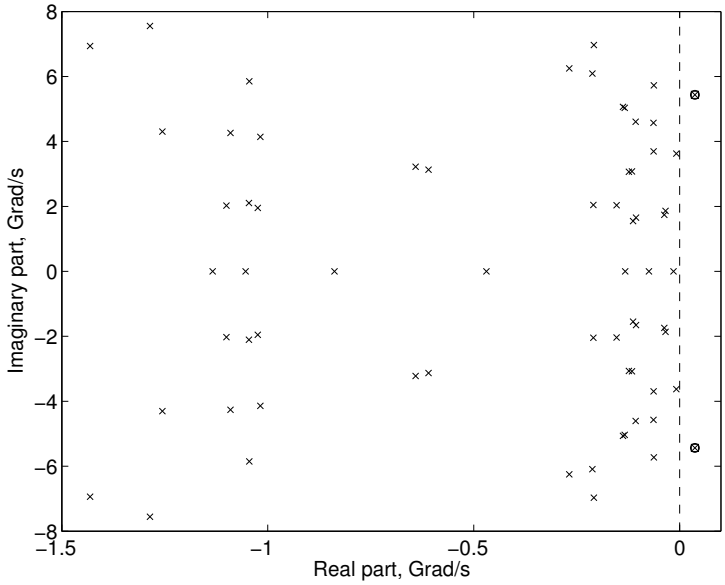

Figure 12: Poles of the complete network with the identical scalar termination designed in band III. Unstable poles are highlighted with a circle.

As a further illustration of the loss of stability, we show in Figure 13 the transient response excited in the complete network with the band III design of identical scalar terminations. The transient response has been obtained with SPICE on a simulation deck obtained by synthesizing the termination as in Table 1. For this particular case, each scalar load has been synthesized with structure $R_1||(R_2 + sL)$, with component values $R_1 = 1.93\text{k}\Omega$, $R_2 = 1.29\Omega$, $L = 9.18$ nH. A current source $i_s(t) = e^{\alpha t}\cos(\omega_0 t)u(t)$ in parallel to one of the macromodel ports is used to excite the unstable mode in the network, with $\alpha < 0$ and with ω_0 corresponding to the resonant frequency of the unstable pole. The exponential blow up of the network demonstrates the macromodel destabilization.

This example tells us that passivity is a fundamental property that must be insured in any data processing and modeling step. When passivity is lost (in this case during measurement), obvious difficulties may arise if no proper countermeasures are taken. Note also that stability loss occurs with terminations made of standard circuit elements, having quite realistic component values.

6.2 Delay-based macromodel

We consider now a delay-based macromodel of a transmission line. The structure under investigation, depicted in Fig. 14, is a three-layer flexible interconnect typically used in foldable mobile phones to connect modules residing in different moving blocks [30]. The transmission line is fully characterized once the per-unit-length impedance $\boldsymbol{Z}(s)$ and admittance $\boldsymbol{Y}(s)$ matrices are known, e.g., via quasi-static 2D field solutions in the transverse plane. It is well-known

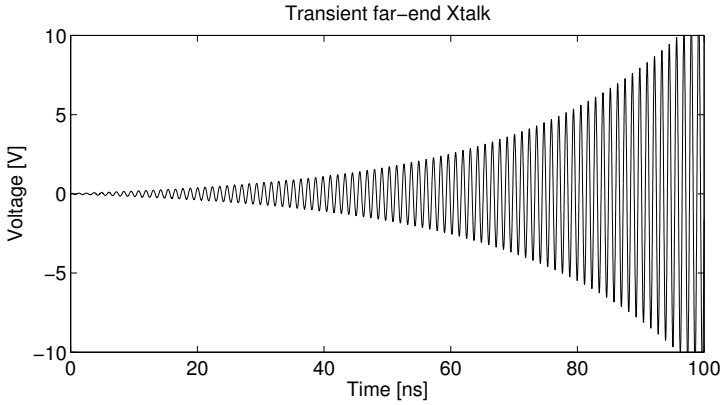

Figure 13: Exponential instability of the terminated network.

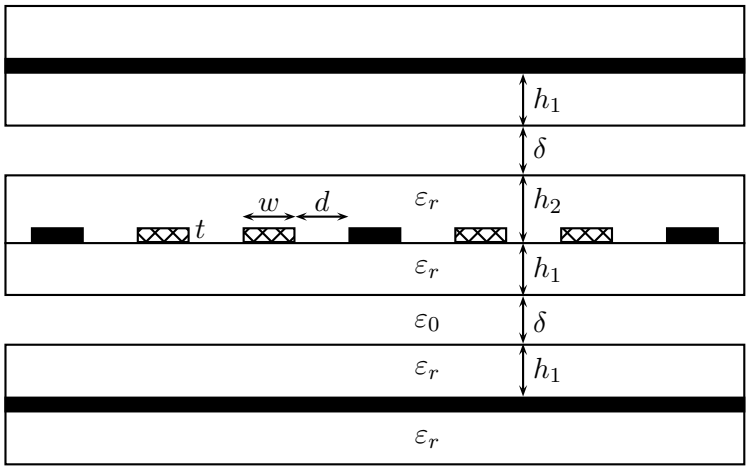

Figure 14: Cross-section of the transmission-line under investigation. Crosshatch and solid fill indicate signal and ground conductors, respectively. Parameter values are $h_1 = 50\,\mu$m, $h_2 = 57.5\,\mu$m, $\delta = 0.5\,$mm, $w = d = 100\,\mu$m, $t = 17.5\,\mu$m, $\varepsilon_r = 3.6$, $\mathcal{L} = 30\,$cm.

that these matrices have a complex dependence on frequency due to skin/proximity effects and dielectric losses [25]. This makes a direct inclusion of such models in standard SPICE-based solvers difficult [1].

A macromodel for this structure can be derived in closed-form from the Telegrapher's equations using the Generalized Method of Characteristics [30, 31]. The resulting macromodel equations are

$$\begin{aligned} \boldsymbol{I}_1 &= \boldsymbol{Y}_c(s)\boldsymbol{V}_1 - \boldsymbol{Q}(s)\ (\boldsymbol{Y}_c(s)\boldsymbol{V}_2 + \boldsymbol{I}_2) \\ \boldsymbol{I}_2 &= \boldsymbol{Y}_c(s)\boldsymbol{V}_2 - \boldsymbol{Q}(s)\ (\boldsymbol{Y}_c(s)\boldsymbol{V}_1 + \boldsymbol{I}_1) \end{aligned} \tag{56}$$

where $\boldsymbol{V}_1, \boldsymbol{I}_1$ and $\boldsymbol{V}_2, \boldsymbol{I}_2$ denote the near and far end terminal voltage and current vectors, with $\boldsymbol{Y}_c(s)$, $\boldsymbol{Q}(s)$ being the characteristic admittance and the propagation operator, respectively, defined as

$$\boldsymbol{\Gamma}^2(s) = \mathbf{Y}(s)\mathbf{Z}(s)\,, \qquad \mathbf{Y}_c(s) = \boldsymbol{\Gamma}^{-1}(s)\mathbf{Y}(s)\,, \qquad \mathbf{Q}(s) = e^{-\mathcal{L}\boldsymbol{\Gamma}(s)}\,. \tag{57}$$

Due to the complex dependence of $\boldsymbol{Y}_c(s)$ and $\boldsymbol{Q}(s)$ on frequency, a rational approximation combined with modal delay extraction is performed

$$\boldsymbol{Y}_c(s) \simeq \sum_n \frac{\boldsymbol{R}_n^Y}{s - p_n} + \boldsymbol{Y}_\infty\,, \quad \boldsymbol{Q}(s) \simeq \boldsymbol{M}\, e^{-s\boldsymbol{T}} \left(\sum_n \frac{\boldsymbol{R}_n^P}{s - q_n} + \boldsymbol{P}_\infty \right) \boldsymbol{M}^{-1} \tag{58}$$

in order to implement the model as a SPICE-compatible stamp, i.e., as a set of delayed ordinary differential equations. The delay matrix $\boldsymbol{T}$ is diagonal, and the constant matrix $\boldsymbol{M}$ collects the line modal profiles at $s = \infty$. More details can be found in [31]. We remark that (56) defines only implicitly the macromodel, but the corresponding scattering matrix $\boldsymbol{H}(s)$ (not reported here) can be readily obtained using simple algebraic calculations from (56). Despite the very recent results of [26, 27, 28], passivity enforcement of such macromodels still remains an open problem, due to the presence of the delay terms.

Since the structure is a transmission line, any practical termination scheme never couples directly the near-end and the far-end ports. Therefore, only the passivity of the model under structured terminations with reduced coupling is important. The structured singular value norms have been computed for the "identical scalar", "scalar", and "two-block" cases, leading to a maximum value of about 1.00031 for all three cases, in a frequency band between 10 and 20 MHz. Note that the raw data used to derive the model are passive, so that the small passivity violation is introduced during the rational approximation phase.

Application of Algorithm 1 for the "identical scalar" case leads to an unstable pole $s_0 = (1.113 \times 10^4 + j7.226 \times 10^7)\,\mathrm{rad/s}$. The synthesis of the destabilizing load produces a $R_1||(R_2 + sL)$ termination at all ports, with component values $R_1 = 335.4\,\mathrm{k\Omega}$, $R_2 = 7.454\,\mathrm{m\Omega}$, and $L = 0.433\,\mu\mathrm{H}$. A further confirmation of the destabilization process is provided in Fig. 15, where a

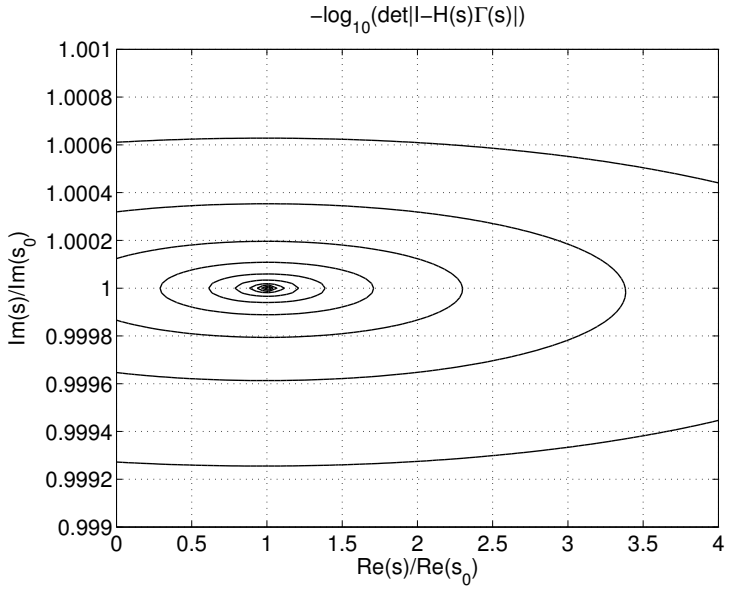

Figure 15: Contour plot of $\log|\det(\boldsymbol{I} - \boldsymbol{H}(s)\boldsymbol{\Gamma}(s))|$ around the location of the destabilizing pole s_0.

contour plot of $\log|\det(\boldsymbol{I} - \boldsymbol{H}(s)\boldsymbol{\Gamma}(s))|$ is depicted as a function of s around the location of the destabilizing pole s_0 in the right-hand complex plane. The crowding of the contour lines pinpoints the expected singularity at $s = s_0$.

6.3 RF amplifier circuit

The last example we consider is a two-port FET-based microwave amplifier circuit. We are interested in the stability properties of the amplifier under variable independent one-port terminations up to 10 GHz. Therefore, we compute the structured singular value for the "scalar" case, as reported in Table 2. The results are depicted in Fig. 16, where also the norm of the scattering matrix and the input-output transmission coefficient H_{21} are reported. Since the structured singular value is uniformly bounded by one in the frequency band of interest (upper bound is 0.99924), the amplifier will remain stable when no external coupling is present between its input and output port. This example shows that, in addition and as a generalization of existing techniques [15]-[21], the structured singular value can be adopted as a single metric for the robust stability assessment of any type of device, including active elements, provided that the specific coupling structure of its terminations is predefined.

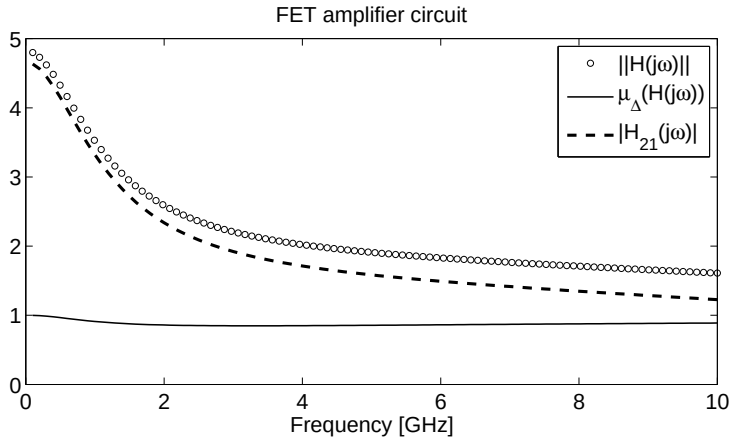

Figure 16: Stability analysis of a two-port RF amplifier circuit. Since the structured singular value $\mu_{\boldsymbol{\Delta}}(\boldsymbol{H}(j\omega))$ for the "scalar" case is less than one, the amplifier remains unconditionally stable for any termination network that does not couple its input and output ports.

Conclusions

In this paper, we have provided an algorithmic procedure for the identification of a particular passive termination that drives a non-passive macromodel to instability. The structure of the termination, from no port coupling to the fully-coupled case, can be chosen almost arbitrarily depending on suitable conditions. These conditions are explicitly derived in each case and involve the unitary boundedness of a suitable norm of the macromodel scattering matrix at the frequency of interest. We remark that there are no important practical limitations on the size of macromodel that can be handled by the proposed algorithms, since the destabilization synthesis is performed at a single working frequency.

The material in this paper provides a quantitative evidence of the paramount importance of passivity in any macromodel to be used on a CAD environment for system analysis and design. In case macromodel passivity is not guaranteed, obvious global stability problems may arise during model simulation. Consequently, there is a strong motivation for further research on passivity enforcement methods. Although several of such techniques are available for small to medium-size lumped models (say, up to ten ports and up to few hundred states) [32]-[44] and for particular classes of small-size delay-dependent models (see, e.g., [26]-[29] and referenfes therein), robust methods are still unavailable for models having large dynamic order and a large number of ports, as typically found, e.g., in high-speed packaging applications. For instance, the generation of accurate broadband passive macromodels of full IC packages for chip-package-board Signal Integrity analysis still remains an open problem due to the overwhelming computational complexity of state of the art techniques.

Acknowledements

The Author is grateful to Prof. Civalleri for his valuable and constructive comments on the manuscript and to Prof. Pirola for providing the RF amplifier example. The Author would also like to thank the anonymous reviewers for their constructive and challenging comments, which helped considerably to improve the quality and the readability of this work.

References

[1] M. Nakhla and R. Achar, "Simulation of High-Speed Interconnects", *Proc. IEEE*, May 2001, Vol. 89, No. 5, pp. 693–728.

[2] M. Celik, L. Pileggi, A. Obadasioglu, *IC Interconnect Analysis*, Kluwer, 2002.

[3] B. Gustavsen, A. Semlyen, "Rational approximation of frequency responses by vector fitting", *IEEE Trans. Power Delivery*, Vol. 14, July 1999, pp. 1052–1061.

[4] R. Gao, S. Mekonnen, W. T. Beyene, J. Schutt-Ainé, "Black-Box Modeling of Passive Systems by Rational Function Approximation", *IEEE Trans. Advanced Packaging*, vol. 28, N. 2, May 2005, pp. 209–215.

[5] G. Csaba, A. Màtyàs, F. Peretti, P. Lugli, "Circuit modelling of coupling between nanosystems and microwave coplanar waveguides," *International Journal of Circuit Theory and Applications*, vol. 35, no. 3, pp. 315-324, 2007.

[6] A. I. Csurgay, "On circuit models for quantum-classical networks," *International Journal of Circuit Theory and Applications*, vol. 35, no. 5-6, pp. 471-484, 2007.

[7] T. J. Brazil, "The modelling and simulation of high-frequency electronic circuits," *International Journal of Circuit Theory and Applications*, vol. 35, no. 5-6, pp. 533-546, 2007.

[8] V. Belevitch, *Classical Network Theory*, Holden-Day, San Francisco, 1968.

[9] M. R. Wohlers, *Lumped and Distributed Passive Networks*, Academic Press, 1969.

[10] D. C. Youla, L. J. Castriota and H. J. Carlin, "Bounded Real Scattering Matrices and the Foundations of Linear Passive Network Theory," *IRE Trans. on Circuit Theory*, vol. CT-6, pp. 102–124, March 1959.

[11] A. H. Zemanian, *Realizability theory for continuous linear systems.* Mathematics in Science and Engineering, Vol. 97, New York - London: Academic Press. XV, 231 p., 1972.

[12] E. S. Kuh and R. A. Rohrer, *Theory of Linear Active Networks*, Holden-Day, 1967.

[13] S. K. Mitra, *Analysis and Synthesis of Linear Active Networks*, Wiley, 1969

[14] R. Spence, *Linear Active Networks*, Wiley, 1970.

[15] J. M. Rollett, "Stability and power-gain invariants of linear two ports," *IRE Trans. Circuit Theory*, vol. CT-9, no. 1, pp. 29-32, Mar. 1962.

[16] M. L. Edwards, "A new criterion for linear two-port stability using a single, geometrically derived parameter," *IEEE Trans. Microw. Theory Tech.*, vol. 40, no. 12, pp. 2303-2311, Dec. 1992.

[17] D. Woods, "Reappraisal of the unconditional stability criteria for active 2-port networks in terms of S parameters," *IEEE Trans. Circuits Syst.*, vol. CAS-23, no. 2, pp. 73-81, Feb.'1976.

[18] M. Olivieri, G. Scotti, P. Tommasino, A. Trifiletti, "Necessary and Sufficient Conditions for the Stability of Microwave Amplifiers With Variable Termination Impedances", *IEEE Transactions on Microwave Theory And Techniques*, Vol. 53, No. 8, Aug. 2005 , pp. 2580–2586.

[19] M. Balsi, M. Olivieri, G. Scotti, P. Tommasino, A. Trifiletti, "Discussion and new proofs of the conditional stability criteria for multidevice microwave amplifiers", *IEE Proceedings on Microwaves, Antennas and Propagation,* Vol. 153, No. 2, Apr. 2006, pp. 177–181.

[20] P. Marietti, G. Scotti, A. Trifiletti, G. Viviani, "Stability Criterion for Two-Port Network With Input and Output Terminations Varying in Elliptic Regions", *IEEE Transactions on Microwave Theory And Techniques*, Vol. 54, No. 12, Dec. 2006, pp. 4049–4055.

[21] P. Bianco, G. Ghione, M. Pirola, "New simple proofs of the two-port stability criterium in terms of the single stability parameter $\mu_1(\mu_2)$ *IEEE Transactions on Microwave Theory And Techniques*, Vol. 49, No. 6, June 2001, pp. 1073–1076.

[22] K. Zhou, J. C. Doyle, K. Glover, *Robust and Optimal Control*, Prentice-Hall, 1996

[23] P. M. Young, J. C. Doyle, "Computation of μ with Real and Complex Uncertainties", Proc. of the 29th Conference on Decision and Control, Honolulu, Hawaii, Dec. 1990, pp. 1230–1235

[24] A. Packard, M. K. H. Fan, J. Doyle, "A power method for the structured singular value", Proc. of the 27th Conference on Decision and Control, Austin, Texas, Dec. 1988, pp. 2132–2137

[25] A. Ege Engin, Wolfgang Mathis, Werner John, Grit Sommer, Herbert Reichl, "Closed-form network representations of frequency-dependent RLGC parameters", *Int. J. Circuit Theory and Applications*, Vol. 33, No. 6, 2005, pp. 463–485.

[26] E. Gad, Changzhong Chen, M. Nakhla, R. Achar, "Passivity Verification in Delay-Based Macromodels of Electrical Interconnects", *IEEE Trans. CAS-I*, Vol. 52, No. 10, Oct. 2005, pp. 2173–2187

[27] E. Gad, C. Chen, M. Nakhla, R. Achar, "A Passivity Checking Algorithm for Delay-Based Macromodels of Lossy Transmission Lines," in *9th IEEE Workshop on Signal Propagation on Interconnects*, 10-13 May 2005, pp. 125–128.

[28] A. Chinea, S. Grivet-Talocia, "A Passivity Enforcement Scheme for Delay-Based Transmission Line Macromodels", *IEEE Microwave and Wireless Components Letters*, 2007, in press.

[29] Qing-Long Han, "Stability analysis for a partial element equivalent circuit (PEEC) model of neutral type", *Int. J. Circuit Theory and Applications*, Vol. 33, No. 4, 2005, pp. 321–332.

[30] S. Grivet-Talocia, S. Acquadro, M. Bandinu, F. G. Canavero, I. Kelander, and M. Rouvala, "A parameterization scheme for lossy transmission line macromodels with application to high speed interconnects in mobile devices," *IEEE Trans. Electromagnetic Compatibility*, vol. 49, pp. 18–24, February 2007.

[31] S. Grivet-Talocia, H. M. Huang, A. E. Ruehli, F. Canavero, I. M. Elfadel, "Transient Analysis of Lossy Transmission Lines: an Effective Approach Based on the Method of Characteristics" , *IEEE Trans. Advanced Packaging*, pp. 45–56, vol. 27, n. 1, Feb. 2004.

[32] S. Boyd, L. El Ghaoui, E. Feron, V. Balakrishnan, *Linear matrix inequalities in system and control theory*, *SIAM studies in applied mathematics*, SIAM, Philadelphia, 1994.

[33] C.P.Coelho, J.Phillips, L.M.Silveira, "A Convex Programming Approach for Generating Guaranteed Passive Approximations to Tabulated Frequency-Data", *IEEE Trans. Computed-Aided Design of Integrated Circuits and Systems*, Vol. 23, No. 2, February 2004.

[34] H. Chen, J. Fang, "Enforcing Bounded Realness of S parameter through trace parameterization", in *12th IEEE Topical Meeting on Electrical Performance of Electronic Packaging*, October 27–29, 2003, Princeton, NJ, pp. 291–294.

[35] Bogdan Dumitrescu, "Parameterization of Positive-Real Transfer Functions With Fixed Poles", *IEEE Trans. CAS-I*, vol. 49, n. 4, April 2002, pp. 523-526.

[36] B. Gustavsen, A. Semlyen, "Enforcing passivity for admittance matrices approximated by rational functions", *IEEE Trans. Power Systems*, Vol. 16, 2001, 97–104.

[37] D. Saraswat, R. Achar and M. Nakhla, "A Fast Algorithm and Practical Considerations For Passive Macromodeling Of Measured/Simulated Data", *IEEE Transactions on Components, Packaging and Manufacturing Technology*, Vol. 27, pp. 57–70, Feb. 2004.

[38] S. Grivet-Talocia, "Enforcing Passivity of Macromodels via Spectral Perturbation of Hamiltonian Matrices," in *7th IEEE Workshop on Signal Propagation on Interconnects, Siena, Italy*, May 11–14, 2003, pp. 33–36.

[39] D. Saraswat, R. Achar, M. Nakhla, "Enforcing Passivity for Rational Function Based Macromodels of Tabulated Data", in *12th IEEE Topical Meeting on Electrical Performance of Electronic Packaging*, October 27–29, 2003, Princeton, NJ, pp. 295–298.

[40] D. Saraswat, R. Achar and M. Nakhla, "Global Passivity Enforcement Algorithm for Macromodels of Interconnect Subnetworks Characterized by Tabulated Data", *IEEE Transactions on VLSI Systems*, Vol. 13, No. 7, pp. 819–832, July 2005.

[41] S. Grivet-Talocia, "Passivity enforcement via perturbation of Hamiltonian matrices", *IEEE Trans. CAS-I*, pp. 1755-1769, vol. 51, n. 9, September, 2004

[42] S. Grivet-Talocia, A. Ubolli "On the Generation of Large Passive Macromodels for Complex Interconnect Structures", *IEEE Trans. Adv. Packaging*, vol. 29, No. 1, pp. 39–54, Feb. 2006

[43] S. Grivet-Talocia, "Improving the efficiency of passivity compensation schemes via adaptive sampling", *14th IEEE Topical Meeting on Electrical Performance of Electronic Packaging*, Austin, Texas (USA), October 24–26, 2005, pp. 231–234.

[44] A Lamecki and M. Mrozowski, "Equivalent SPICE Circuits With Guaranteed Passivity From Nonpassive Models," IEEE Transactions on Microwave Theory And Techniques, Vol. 55, No. 3, March 2007, pp. 526–532.